Angewandte Chemie
Eine Zeitschrift der Gesellschaft Deutscher Chemiker

Supporting Information

69451 Weinheim, Germany

Modifying Alkylzinc Reactivity with 2,2′-Dipyridylamide: Activation of *t*Bu–Zn Bonds for *para*-Alkylation of Benzophenone**

David R. Armstrong, Jennifer A. Garden, Alan R. Kennedy, Robert E. Mulvey, and Stuart D. Robertson*

anie_201302426_sm_miscellaneous_information.pdf

Table of Contents

Table of Figures

Additional Crystal Information

Table 1 Crystallographic data and refinement details for compounds **2**-**5**.

Compound	**2**	**3**	**4**	**5**
Empirical formula	$C_{28}H_{34}N_6Zn_2$	$C_{40}H_{66}N_{10}Na_2Zn$	$C_{50}H_{92}N_3NaO_6Zn_2$	$C_{50}H_{92}KN_3O_6Zn_2$
M_r (g mol^{-1})	585.35	798.38	985.00	1001.11
Crystal system	Monoclinic	Monoclinic	Triclinic	Triclinic
Space group	$P2_1/c$	$P2_1/n$	P -1	P-1
a/ Å	9.4833(3)	11.5137(3)	10.0075(11)	9.8787(6)
b/ Å	10.4377(4)	21.6403(4)	11.1283(9)	11.2247(7)
c/ Å	14.0888(5)	18.3837(3)	13.3084(15)	13.5206(7)
α (º)	90	90	69.353(9)	72.296(5)
β (º)	105.844(4)	93.636(2)	85.491(9)	83.032(5)
γ (º)	90	90	84.723(8)	84.558(5)
V/Å^3	1341.58(8)	4571.26(16)	1379.3(2)	1415.02(14)
Z	2	4	1	1
2θmax	58.0	57.9	58.0	60.4
Measured reflections	7483	23176	16565	15934
Unique reflections	3451	10516	6820	7408
R_{int}	0.0284	0.0243	0.0346	0.0309
Observed rflns [$I > 2\sigma(I)$]	2840	8121	5614	5590
μ (mm^{-1})	1.816	0.594	0.922	0.965
No. of parameters	166	492	321	359
R [on *F*, obs rflns only]	0.0413	0.0388	0.0606	0.0642
wR [on F^2, all data]	0.1039	0.0864	0.1679	0.1874
GoF	1.065	1.032	1.057	1.034
Largest diff. peak/hole/e Å^{-3}	1.583/-0.732	0.549/-0.494	0.912/-0.723	0.911/-0.597

Crystallographic Structure of [{(dpa)Zn(*t*Bu)}$_2$], 2

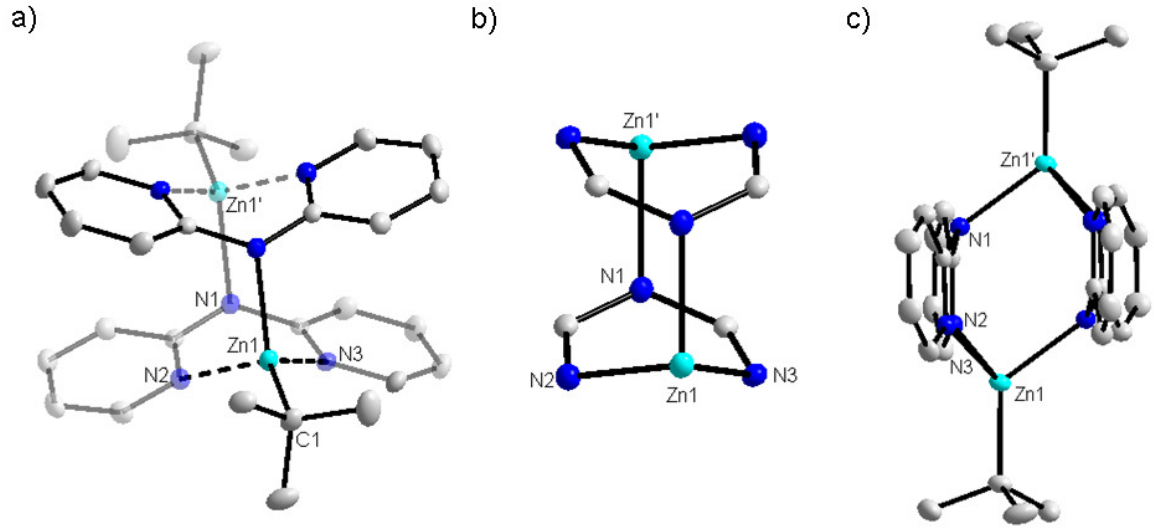

Figure S1 a) Molecular structure of heteroleptic **2** with thermal ellipsoids at 50% probability level and hydrogen atoms omitted for clarity. Selected bond lengths (Å) and angles (°): Zn1-N1, 2.116(2); Zn1-N2, 2.079(2); Zn1-N3, 2.070(2); Zn1-C1, 2.005(3); C1-Zn1-N1, 126.47(10); C1-Zn1-N2, 122.61(10); C1-Zn1-N3, 123.80(10); N1-Zn1-N2, 94.13(8); N1-Zn1-N3, 93.25(8); N2-Zn1-N3, 85.99(8); b) fragment of **2** highlighting the "hourglass" shaped $(NCNCNZn)_2$ core; c) side-on view of **2**.

Crystallographic Structure of [{K(THF)$_6$}$^+${Zn(*t*Bu)$_2$(dpa)Zn(*t*Bu)$_2$}$^-$], 5

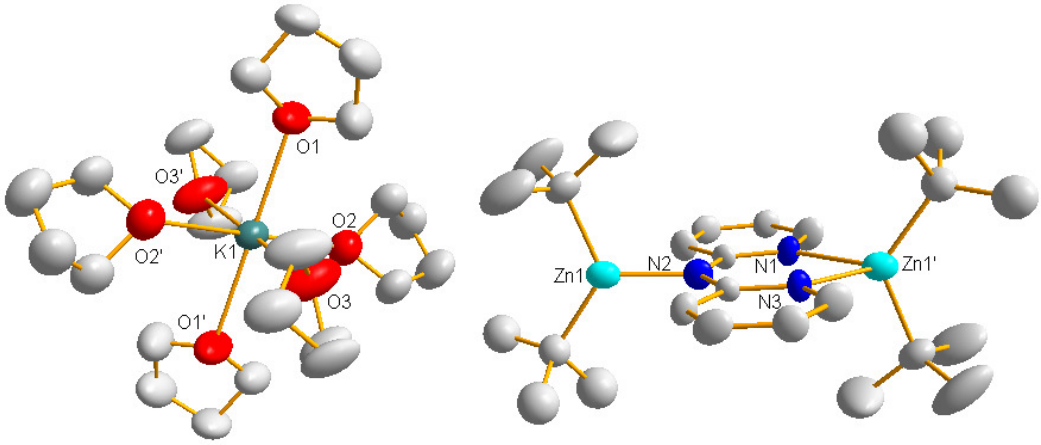

Figure S2 Cation and anion of solvent separated ion pair structure of **5** with thermal ellipsoids at 50% probability level and hydrogen atoms and disorder components omitted for clarity.

Experimental

All reactions were performed under a protective argon atmosphere using standard Schlenk techniques. Hexane, toluene and THF were dried by heating to reflux over sodium benzophenone ketyl and distilled under nitrogen prior to use. BuNa,[1] KCH_2SiMe_3,[2] tBu_2Zn[3] and [(TMEDA)Na(TMP)(*t*Bu)Zn(*t*Bu)], **1**[3] were prepared according to literature methods. NMR spectra were recorded on a Bruker DPX 400 MHz spectrometer, operating at 400.03 MHz for ^{1}H and 100.59 MHz for ^{13}C, or a Bruker DPX 500 MHz spectrometer, operating at 500.13 MHz for ^{1}H and 125.76 MHz for ^{13}C. Dipyridylamine and benzophenone were purchased from Sigma-Aldrich and were used as received.

Synthesis of Crystalline Materials

Synthesis of [{(dpa)Zn(*t*Bu)}$_2$], **2**: M_r = 585.35 g. Dpa(H) (0.34 g, 2 mmol) was dissolved in a mixed hexane (10 mL)/toluene (20 mL) solvent system. This colourless solution was added to a solution of freshly prepared tBu_2Zn (0.36 g, 2 mmol) in hexane (10mL). The resultant pale yellow solution deposited a crop of colourless crystals after 18 h [yield 0.41 g; based upon the dpa(H) stoichiometry, 70%]. ^{1}H NMR (400.03 MHz, C_6D_6, 300K): δ = 7.77 and 7.72 (br. s, 2H, H1-dpa), 7.00 and 6.89 (br. s, 2H, H3-dpa), 6.72 (br. s., 4H, H4-dpa), 6.25 and 5.99 (br. s, 8H, H2-dpa), 1.80 and 1.23 ppm, (br. s, 9H, *t*Bu). ^{13}C NMR (100.59 MHz, C_6D_6, 300K): δ = 163.1 (C5-dpa), 146.6 and 145.5 (C1-dpa), 139.3 (C3-dpa), 137.6 and 122.6 (C4-dpa), 113.9 (C2-dpa), 111.3 (C3-dpa), 35.4 and 33.6 ppm (*t*Bu).

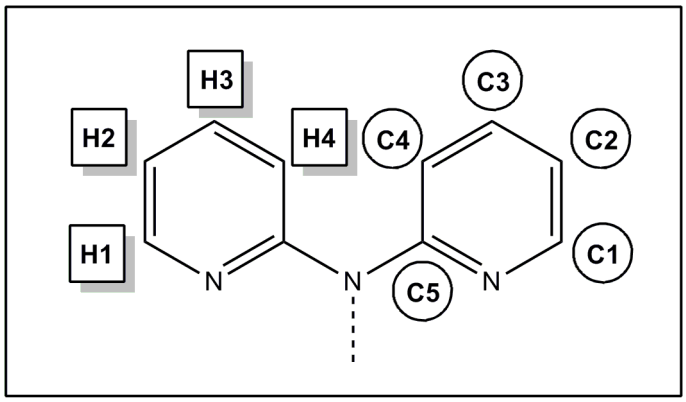

Synthesis of $[(TMEDA)_2Na_2(\mu\text{-}dpa)_2Zn(t\text{Bu})_2]$, **3**: M_r = 798.38 g. TMP(H) (0.34 mL, 2 mmol) was transferred via syringe to a suspension of freshly prepared BuNa (0.16 g, 2 mmol) in hexane (10 mL). The colourless suspension was allowed to stir for 1 hour at ambient temperature. A solution of $t\text{Bu}_2\text{Zn}$ (0.36 g, 2 mmol) in hexane (10 mL) was added to the suspension via cannula, followed by 0.30 mL of TMEDA. Gentle heating produced a pale yellow solution, to which dpa(H) (0.34 g, 2 mmol) was added. This immediately produced a vivid orange solution. The reaction mixture was transferred to the refrigerator (4ºC) where a crop of orange crystals [yield 0.56 g; based upon the dpa(H) stoichiometry, 70%] were deposited after 18 h.

^{1}H NMR (500.13 MHz, C_6D_6, 300K): δ = 8.09 (br. s, 4H, H1-dpa), 7.10 (br. t, 4H, *J*=7.2 Hz, H3-dpa), 6.96 (br. d, *J*=10.5 Hz, 4H, H4-dpa), 6.30 (br. t, 4H, *J*=5.7 Hz, H2-dpa), 1.74 (s, 24H, CH_3-TMEDA) 1.69 (s, 8H, CH_2-TMEDA), 1.57 ppm (br. s, 18H, *t*Bu). ^{13}C NMR (125.76 MHz, C_6D_6, 300K): δ = 165.1 (C5-dpa), 148.9 (C3-dpa), 137.2 (C4-dpa), 113.5 (C1-dpa), 111.2 (C2-dpa), 56.9 (CH_2-TMEDA), 45.5 (CH_3-TMEDA), 35.8 (*t*Bu), 20.7 ppm (quat. *t*Bu).

Synthesis of $[\{Na(THF)_6\}^+\{Zn(t\text{Bu})_2(dpa)Zn(t\text{Bu})_2\}^-]$, **4**: M_r = 985.00 g. A solution of $t\text{Bu}_2\text{Zn}$ (0.36 g, 2 mmol) in hexane (10 mL) was added to a suspension of freshly prepared BuNa (0.16 g, 2 mmol) in hexane (10 mL) via cannula. Dpa(H) (0.34 g, 2 mmol) was added to the resultant solution, producing an orange suspension that was allowed to stir for 20 minutes at ambient temperature. Upon addition of toluene (5 mL) and THF (1.5 mL) an orange solution was produced. Approximately half of the solvent was removed in vacuo and the solution was transferred to the refrigerator

(4ºC). A crop of orange crystals (yield, 0.37 g; 19% out of a maximum of 50% based upon the tBu$_2$Zn stoichiometry) was deposited after 18 h. Labile THF is lost from the crystalline solid upon isolation, which is reflected in low integration values in NMR spectroscopic analyses.

Rational synthesis of [{Na(THF)$_6$}$^+${Zn(tBu)$_2$(dpa)Zn(tBu)$_2$}$^-$]. Dpa(H) (0.34 g, 2 mmol) was added to a freshly prepared suspension of BuNa (0.16 g, 2 mmol) in hexane and the reaction mixture was allowed to stir for 1 hour. A hexane solution of tBu$_2$Zn (0.72 g, 4 mmol) was injected, followed by toluene (5 mL) and THF (1.5 mL), producing an orange solid (yield, 0.41 g; 42% out of a maximum of 100% based on the tBu$_2$Zn stoichiomtery).

^{1}H NMR (500.13 MHz, C_6D_6, 300K): δ = 7.92 (br. s., 2H, H1-dpa), 7.05 (br. s., 2H, H3-dpa), 6.92 (br. s., 2H, H4-dpa), 6.25 (br. s., 2H, H2-dpa), 3.51 (m, 16H, α-THF), 1.39 (m, 16H, β-THF), 1.25 ppm (br. s., 36H, tBu).^{13}C NMR (125.76 MHz, C_6D_6, 300K): δ = 148.3 (C1-dpa), 137.7 (C3-dpa), 113.3 (C4-dpa), 111.7 (C2-dpa), 67.8 (α-THF), 32.8 (tBu), 25.7 (β-THF), 24.8 ppm (tBu quaternary).

Synthesis of [{K(THF)$_6$}$^+${Zn(tBu)$_2$(dpa)Zn(tBu)$_2$}$^-$], **5**: M_r = 1001.11 g. Dpa(H) (0.34 g, 2 mmol) was added to a freshly prepared suspension of K(CH_2SiMe_3) (0.25 g, 2 mmol) in hexane (10 mL). TMEDA (0.60 mL, 4 mmol) was added to this beige suspension. Approximately half of the solvent was removed in vacuo and THF (10 mL) was added to produce a yellow-orange solution. tBu$_2$Zn (0.36 g, 2mmol) in hexane (10 mL) was introduced and the resultant orange solution was transferred to the freezer, where a crop of orange crystals (yield 0.27 g; 14% out of a maximum of 50% based upon the tBu$_2$Zn stoichiometry) was deposited after 72 h. Labile THF is lost from the crystalline solid upon isolation, which is reflected in low integration values in NMR spectroscopic analyses.

^{1}H NMR (400.03 MHz, C_6D_6, 300K): δ = 8.04 (br. s., 2H, H1-dpa), 7.05 (br. t., 2H, H3-dpa), 6.76 (br. d., 2H, H4-dpa), 6.27 (br. t., 2H, H2-dpa), 3.45 (br. s, 15H, α-THF), 1.39 (m, 15H, β-THF), 1.36 (br. s, 36H, tBu). ^{13}C NMR (100.59 MHz, C_6D_6, 300K): δ = 148.1 (C1-dpa), 137.6 (C3-dpa), 115.1 (C4-dpa), 111.7 (C2-dpa), 67.8 (α-THF), 34.2 (tBu), 25.7 (β-THF) and 23.0 ppm (quat. tBu).

Benchmark reactivity studies: nucleophilic addition towards benzophenone

Method A - Work-Up Procedure

To the reaction mixture, deionised water (10 mL), 2 M HCl (20 mL) and diethyl ether (20 mL) were added. The organic layer was separated from the aqueous layer and the aqueous layer was washed with diethyl ether/hexane (3 x 20 mL). Magnesium sulfate was used to dry the combined organic layers. Solvent was removed in vacuo and the crude residue was spiked with 10 mol % hexamethylbenzene [0.0162 g, 0.1 mmol for 1 mmol scale (stoichiometric) reactions; 0.081 g, 0.5 mmol for 5 mmol scale (catalytic) reactions]. ^{1}H NMR spectroscopic analysis was performed and the relative yields of 2- and 4-*tert*-butylbenzophenone, benzhydrol and diphenyl-*tert*-butylmethanol were determined by relative integration. Spectroscopic data show resonances that are in good agreement with the reference standard of a commercially available sample of 4-*tert*-butylbenzophenone.

Stoichiometric Reactions

Control Reaction

A standard solution of tBu$_2$Zn (2 mL of a 0.5 M solution in hexane, 1 mmol) was transferred to a Schlenk flask under argon atmosphere. A further 6 mL of hexane was added, followed by benzophenone (0.18 g, 1 mmol). The reaction mixture was allowed to stir at ambient temperature for 18 h prior to work-up as per Method A.

Donor Amines

A standard solution of tBu$_2$Zn (2 mL of a 0.5 M solution in hexane, 1 mmol) was transferred to a Schlenk flask under argon atmosphere, followed by 6 mL of hexane. Subsequently, a donor amine (either pyridine, 0.16 mL, 2 mmol or TMEDA, 0.15 mL, 1 mmol) was added. Upon addition of pyridine an orange solution was immediately

produced. Benzophenone (0.18 g, 1 mmol) was then added and the reaction mixture was allowed to stir for 18 h at ambient temperature prior to work-up as per Method A.

[(TMEDA)Na(TMP)(*t*Bu)Zn(*t*Bu)], 1

Crystalline sodium zincate **1** (0.46 g, 1 mmol) was dissolved in hexane (8 mL) to produce a primrose solution. Benzophenone (0.18 g, 1 mmol) was added, producing a vivid colour change to emerald green. The reaction mixture was stirred at ambient temperature for 18 h, prior to work up as per Method A.

[(TMEDA)$_2$Na$_2$(μ-dpa)$_2$Zn(*t*Bu)$_2$], 3

BuNa (0.16 g, 2 mmol) was suspended in hexane (6 mL) and dpa(H) (0.34g, 2 mmol) was added. The resultant beige suspension was allowed to stir for 45 minutes at ambient temperature. To this, TMEDA was injected (0.30 mL, 2 mmol), followed by a hexane solution of *t*Bu$_2$Zn (2 mL of a 0.5 M solution, 1mmol). Benzophenone (0.18 g, 1 mmol) was subsequently added and the reaction was stirred at ambient temperature for 18 h, over which time a colour change from orange to green was observed. The reaction was worked up according to Method A.

[{Na(THF)$_6$}$^+${Zn(*t*Bu)$_2$(dpa)Zn(*t*Bu)$_2$}$^-$], 4

Crystalline sodium zinczincate **4** (0.99 g, 1 mmol) was suspended in hexane (8 mL). To this, benzophenone (0.18g, 1 mmol) was added and the reaction mixture was stirred for 18 h at ambient temperature prior to work-up following the procedure outlined in Method A.

Catalytic Reactions

Control Reaction

For control purposes, a standard solution of *t*Bu$_2$Zn (10 mL of a 0.5 M solution in hexane, 5 mmol) was transferred to a Schlenk flask under argon atmosphere. A

further 30 mL of hexane was added, followed by benzophenone (0.90 g, 5 mmol). The reaction mixture was allowed to stir for 18 h under reflux conditions prior to work-up as per Method A.

10 mol % [(TMEDA)Na(TMP)]

BuNa (0.04g, 0.5 mmol) was suspended in hexane (30 mL). TMPH (0.09 mL, 0.5 mmol) was added and the reaction mixture was allowed to stir for 45 minutes. Subsequently, *t*Bu_2Zn (10 mL of a 0.5 M solution of *t*Bu_2Zn in hexane, 5 mmol), TMEDA (0.08 mL, 0.5 mmol), and benzophenone (0.90 g, 5 mmol) were added. The reaction mixture was stirred under reflux conditions for 18h, prior to work-up according to Method A.

10 mol % [(TMEDA)Na(dpa)]$_2$

BuNa (0.08 g, 1 mmol) was suspended in hexane (30 mL) and dpa(H) (0.17g, 1 mmol) was added. The resultant beige suspension was allowed to stir for 45 minutes at ambient temperature. To this, TMEDA was injected (0.15 mL, 1 mmol), followed by a hexane solution of *t*Bu_2Zn (10 mL of a 0.5 M solution, 5mmol). Benzophenone (0.90 g, 5 mmol) was added and the reaction mixture was allowed to stir for 18 h under reflux conditions, prior to work-up as per Method A.

10 mol % [{Na(THF)$_6$$^+$}{Zn(*t*Bu)$_2$(dpa)Zn(*t*Bu)$_2$}$^-$]

Sodium zinczincate **4** (0.49g, 0.5 mmol) was suspended in hexane (30 mL) and a hexane solution of *t*Bu_2Zn was injected (10 mL of a 0.5 M solution of *t*Bu_2Zn in hexane, 5 mmol). Following the addition of benzophenone (0.90 g, 5 mmol), the reaction was stirred for 18 h under reflux conditions, prior to work-up following Method A.

NMR Spectra

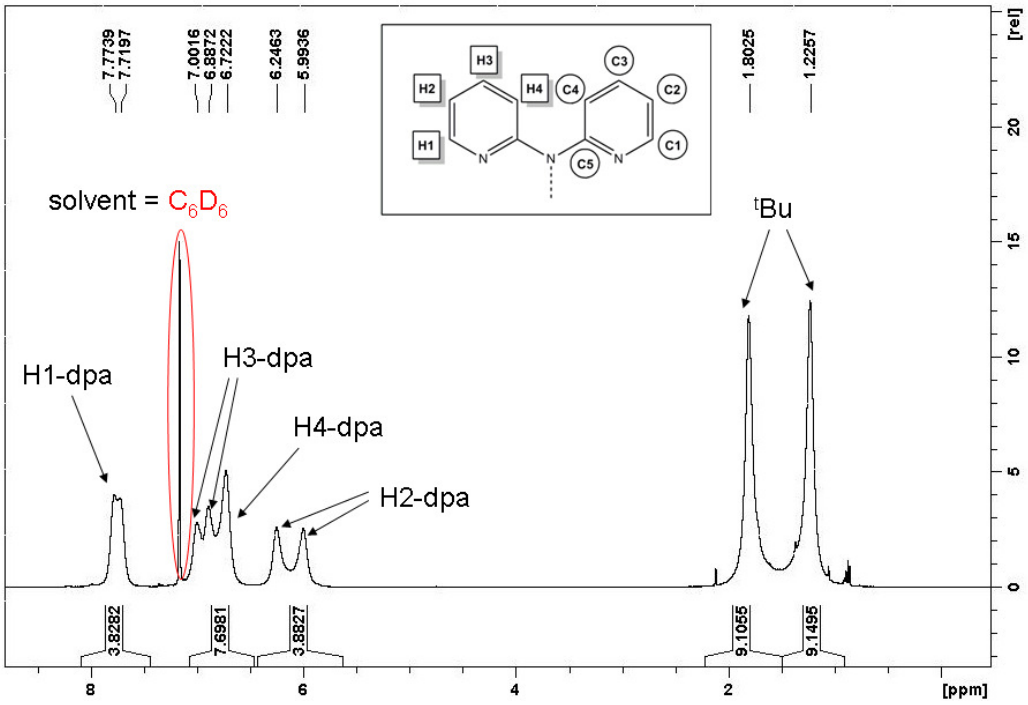

Figure S3 ^{1}H NMR Spectrum of [{(dpa)Zn(*t*Bu)}$_2$] (**2**).

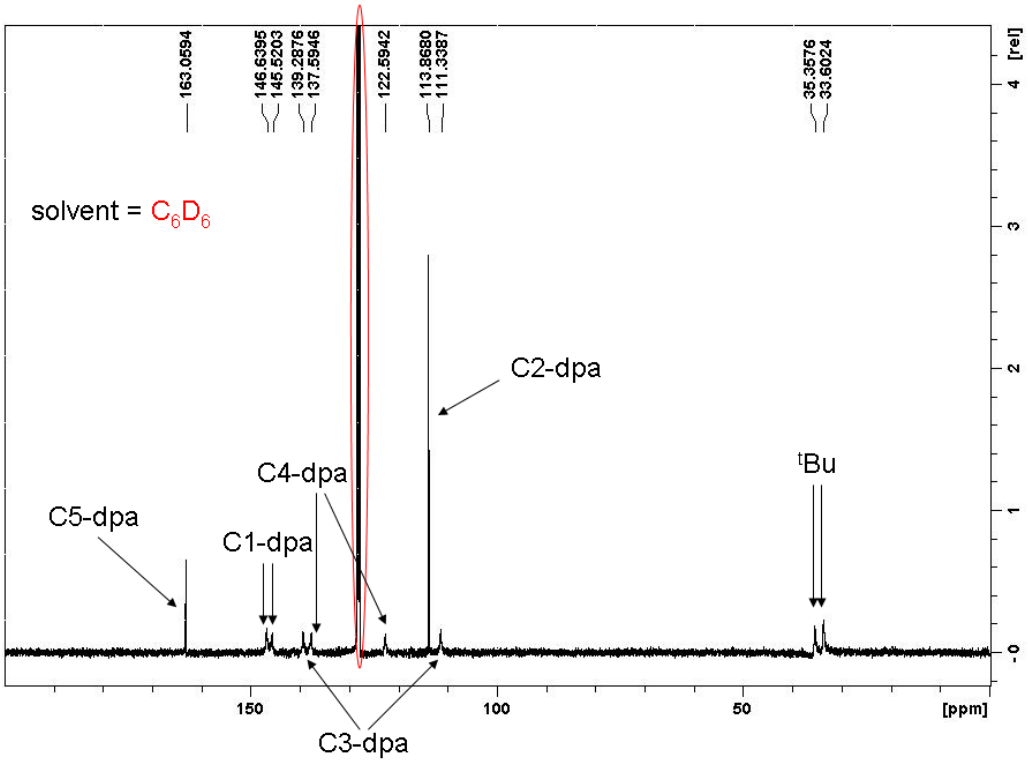

Figure S4 ^{13}C NMR Spectrum of [{(dpa)Zn(*t*Bu)}$_2$] (**2**).

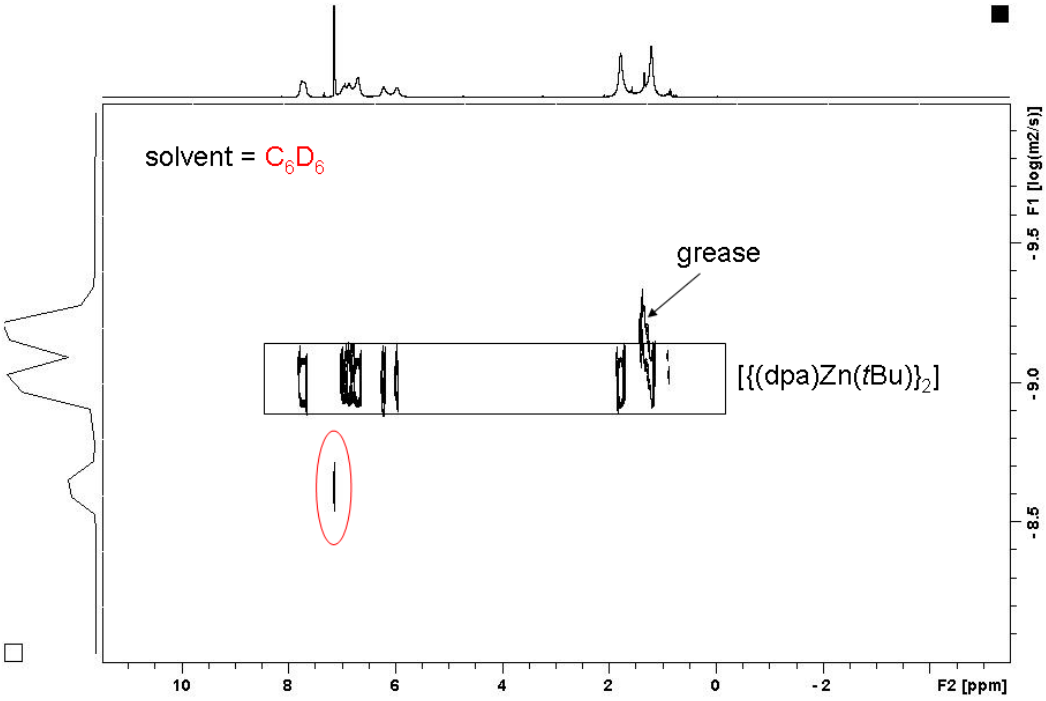

Figure S5 DOSY NMR Spectrum of [{(dpa)Zn(*t*Bu)}$_2$] (**2**).

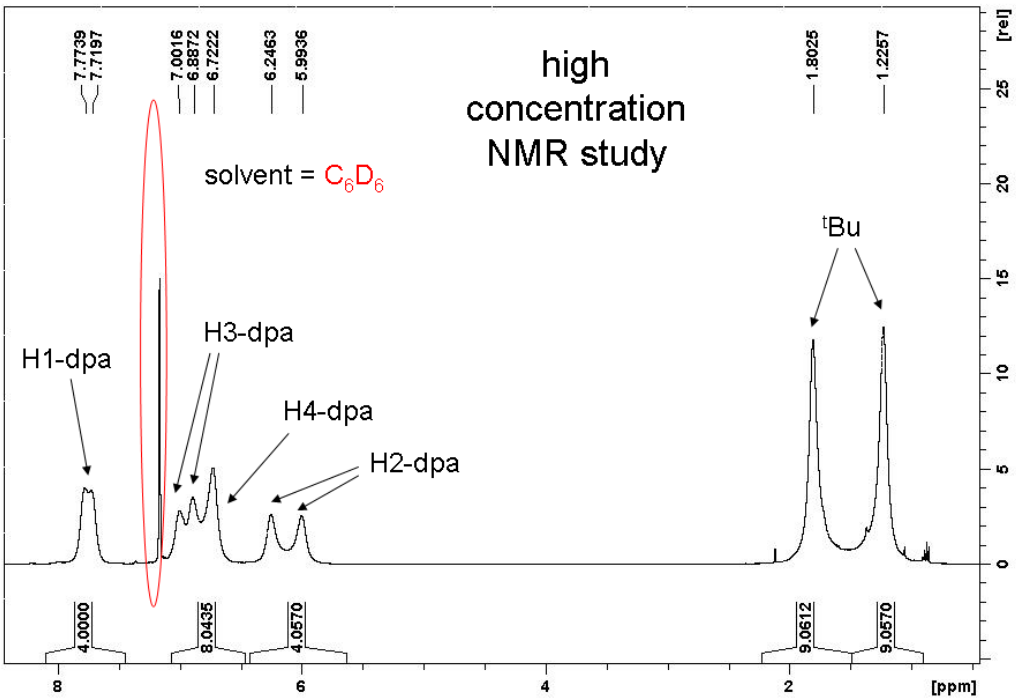

Figure S6 High concentration ^{1}H NMR spectrum of [{(dpa)Zn(*t*Bu)}$_2$] (**2**).

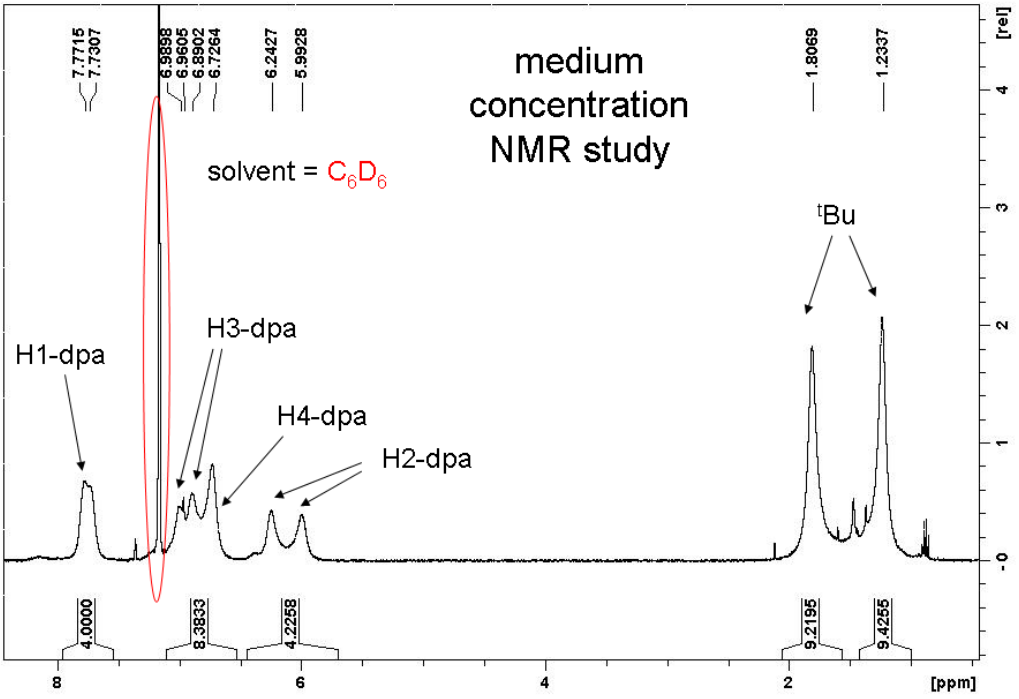

Figure S7 Medium concentration ^{1}H NMR spectrum of [{(dpa)Zn(*t*Bu)}$_2$] (**2**).

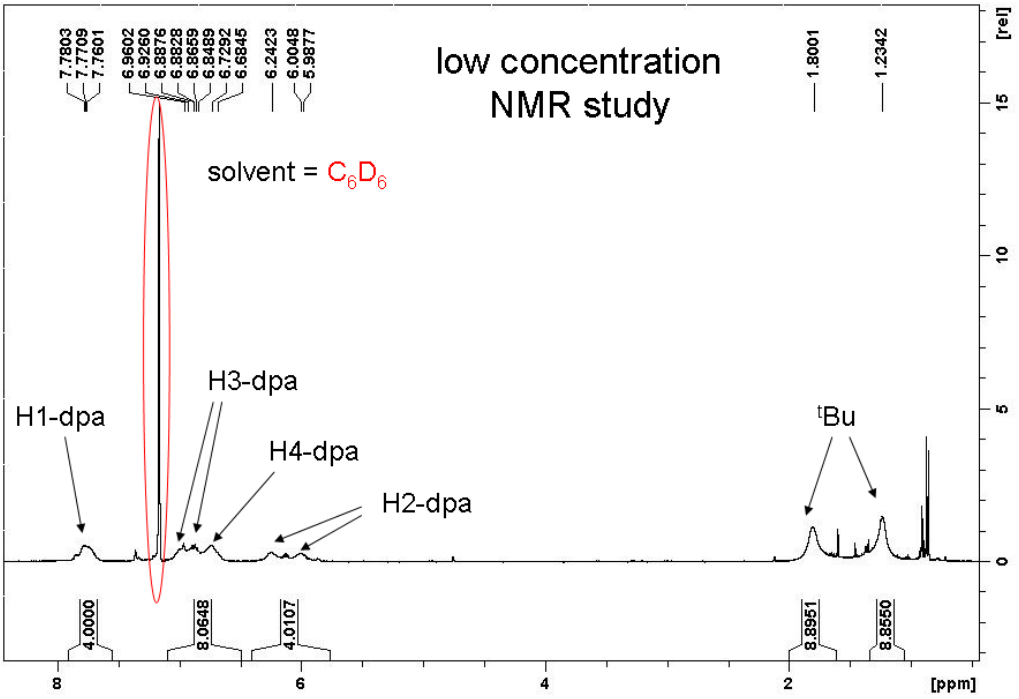

Figure S8 Low concentration ^{1}H NMR spectrum of [{(dpa)Zn(*t*Bu)}$_2$] (**2**).

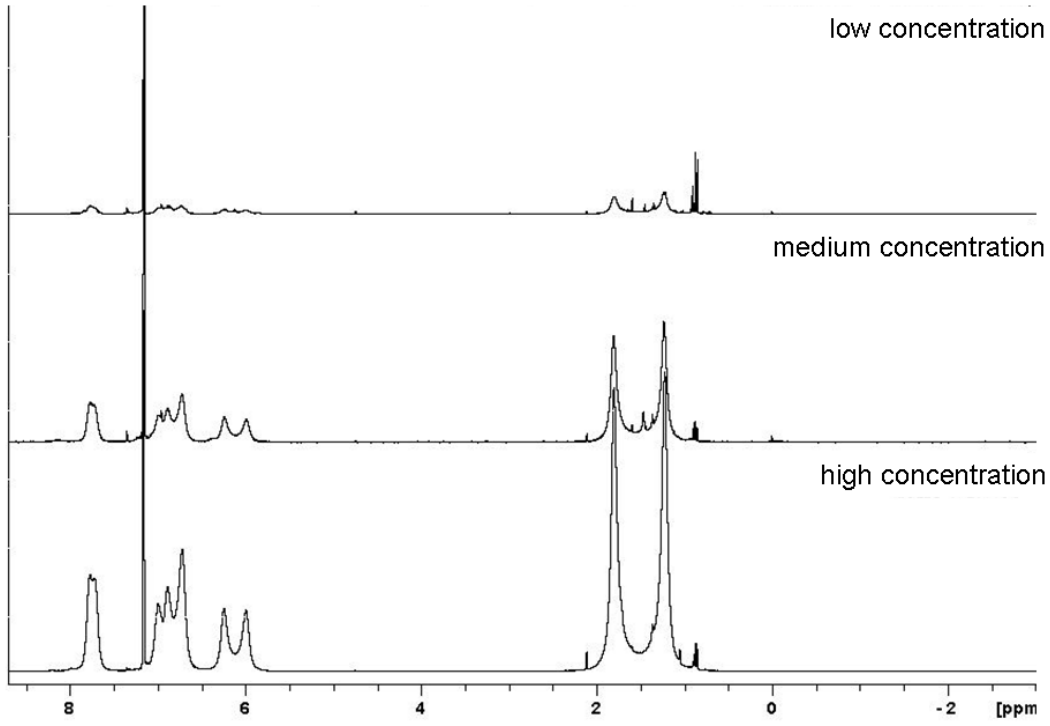

Figure S9 Variable concentration ^{1}H NMR spectra of [{(dpa)Zn(*t*Bu)}$_2$] (**2**).

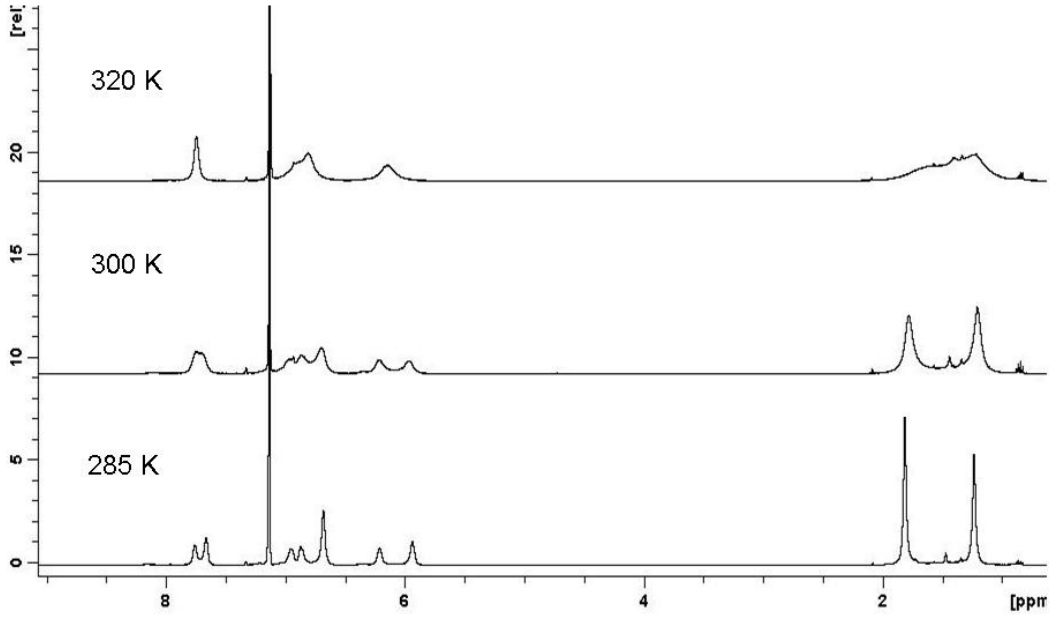

Figure S10 Variable temperature ^{1}H NMR spectra of [{(dpa)Zn(*t*Bu)}$_2$] (**2**) in C_6D_6 solvent.

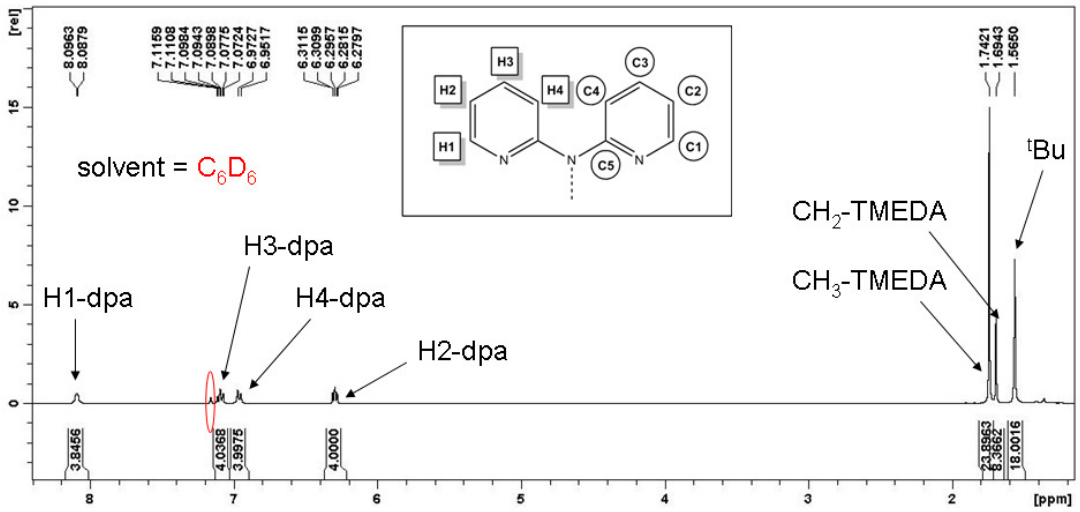

Figure S11 ^{1}H NMR Spectrum of [(TMEDA)$_2$Na$_2$(μ-dpa)$_2$Zn(*t*Bu)$_2$] (**3**).

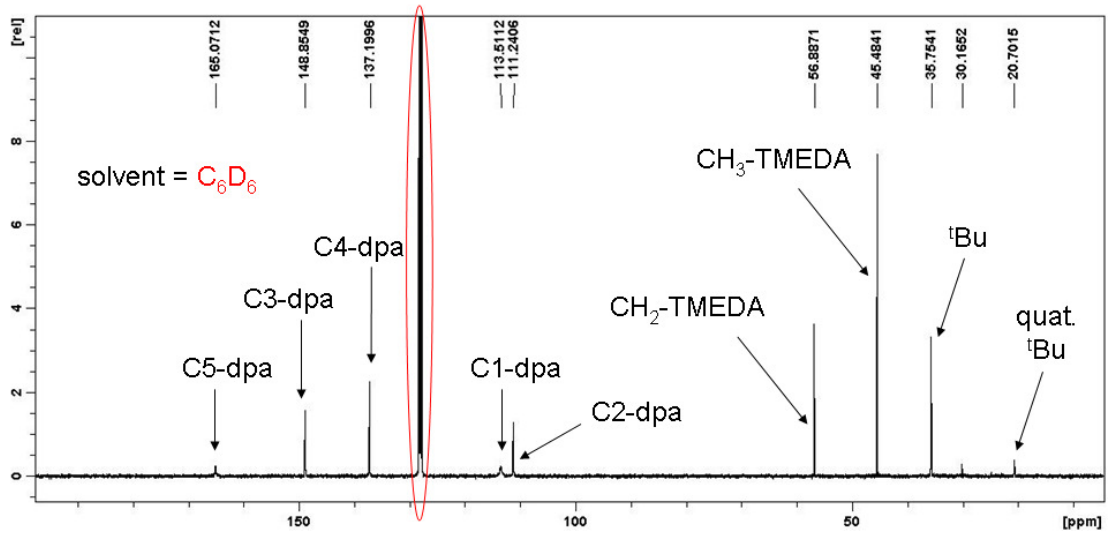

Figure S12 ^{13}C NMR Spectrum of [(TMEDA)$_2$Na$_2$(μ-dpa)$_2$Zn(*t*Bu)$_2$] (**3**).

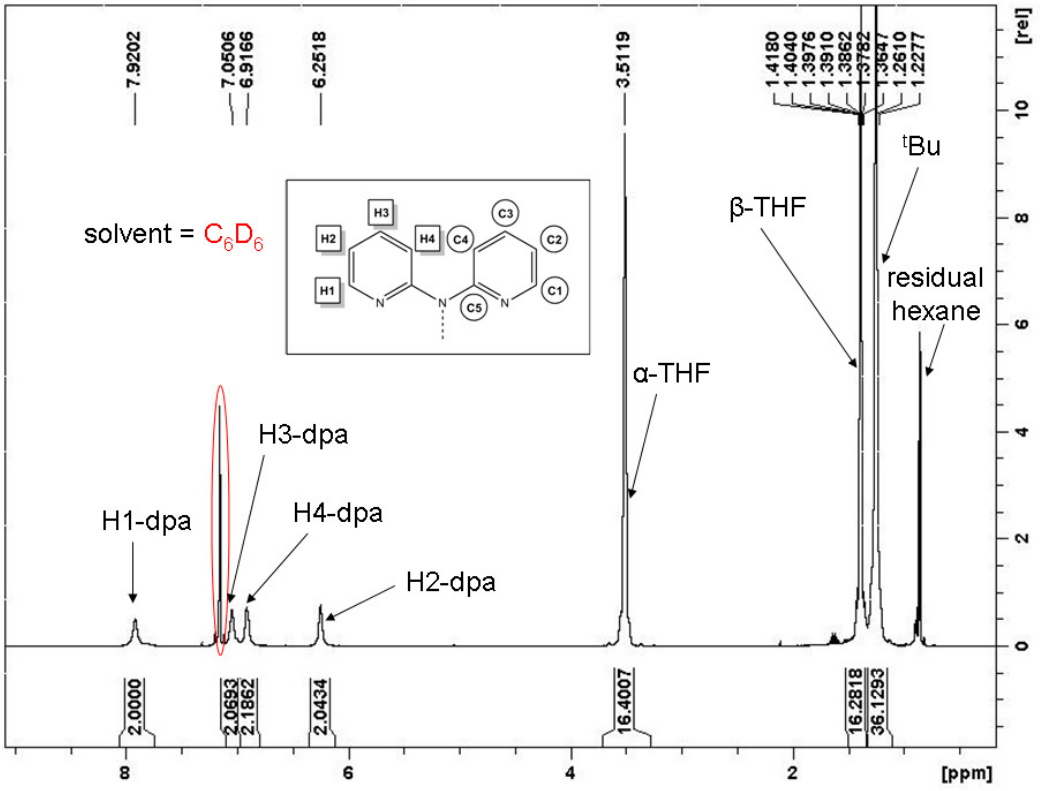

Figure S13 ^{1}H NMR Spectrum of [{Na(THF)$_6$}$^+${Zn(*t*Bu)$_2$(dpa)Zn(*t*Bu)$_2$}$^-$] (**4**).

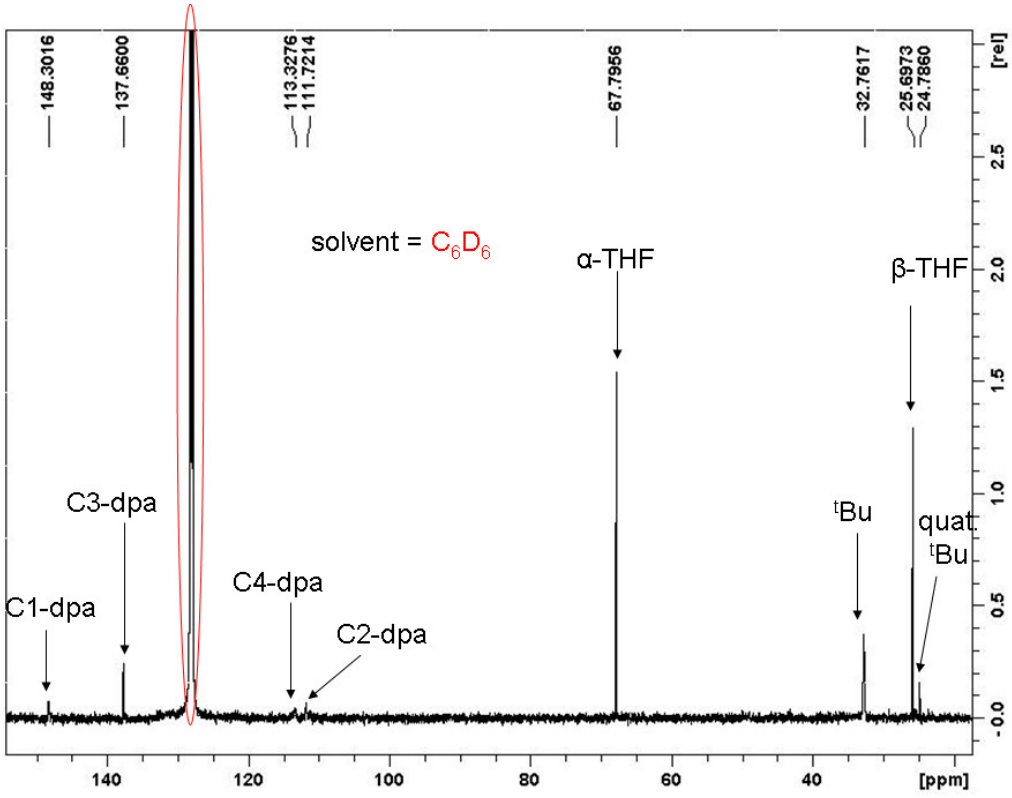

Figure S14 ^{13}C NMR Spectrum of [{Na(THF)$_6$}$^+${Zn(*t*Bu)$_2$(dpa)Zn(*t*Bu)$_2$}$^-$] (**4**).

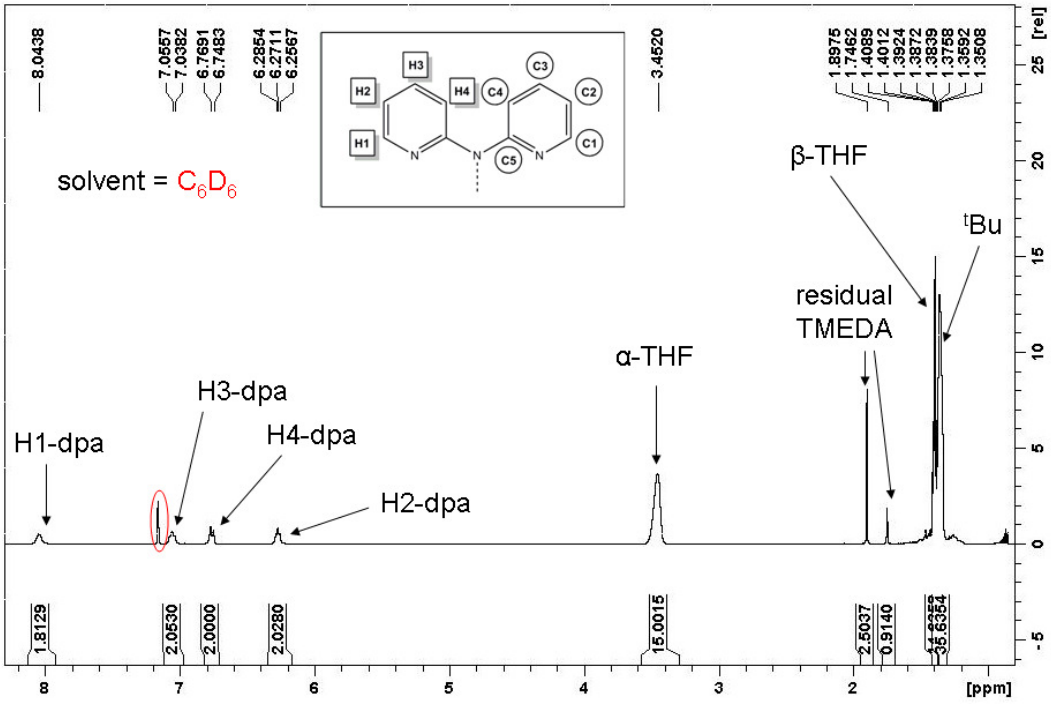

Figure S15 ^{1}H NMR Spectrum of [{K(THF)$_6$}$^+${Zn(*t*Bu)$_2$(dpa)Zn(*t*Bu)$_2$}$^-$] (**5**).

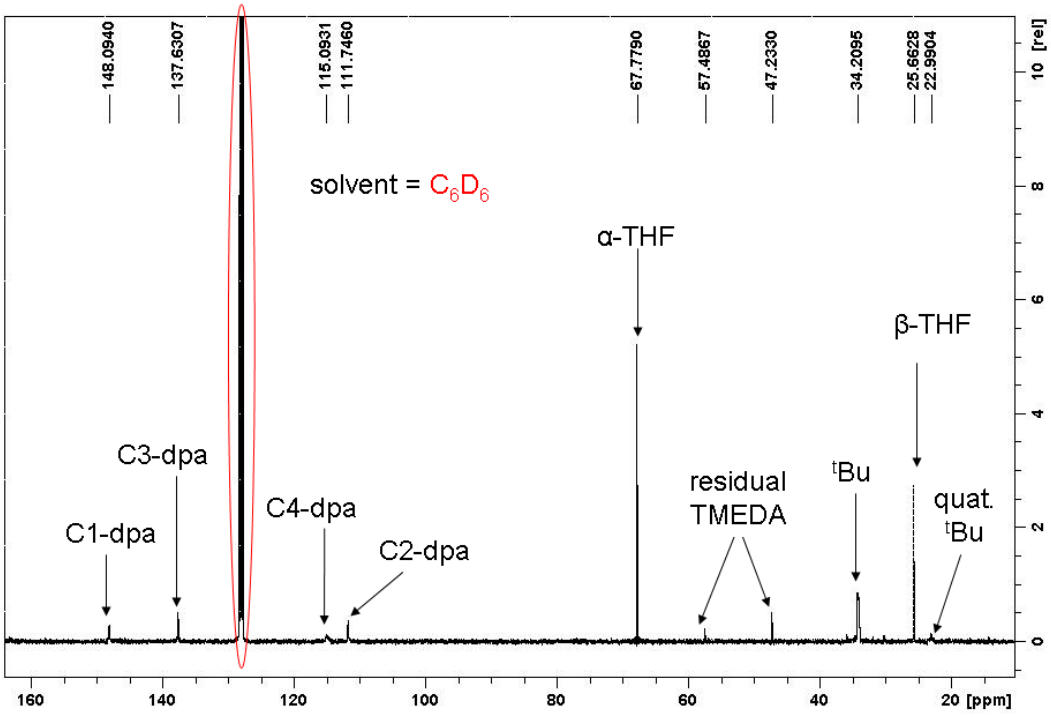

Figure S16 ^{13}C NMR Spectrum of [{K(THF)$_6$}$^+${Zn(*t*Bu)$_2$(dpa)Zn(*t*Bu)$_2$}$^-$] (**5**).

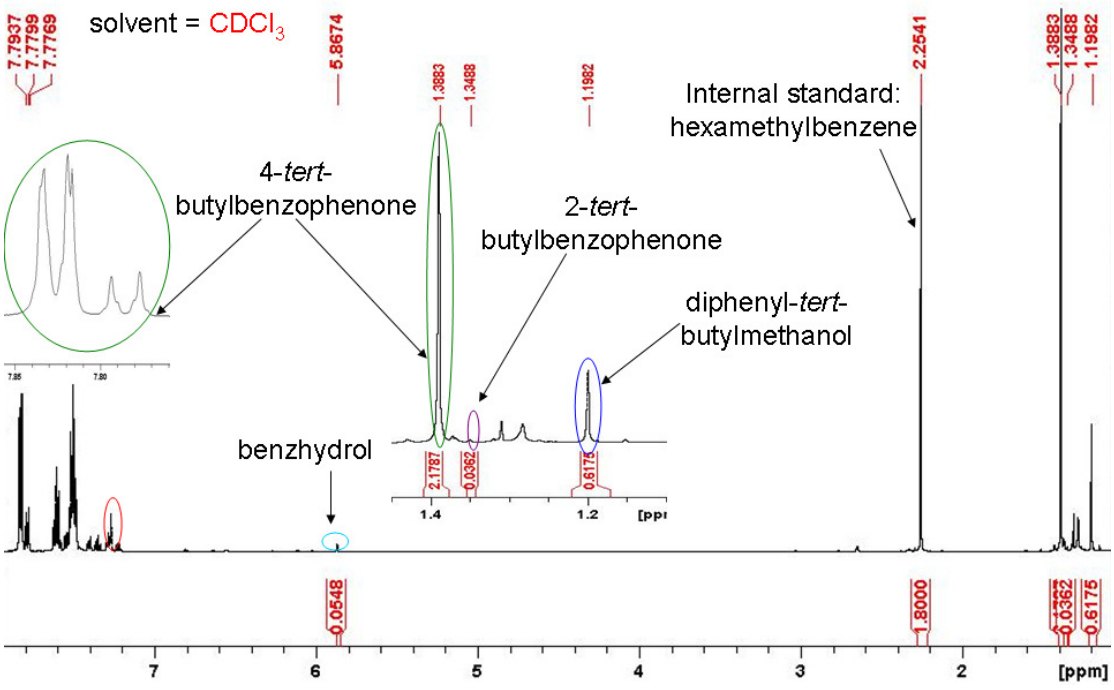

Figure S17 Crude NMR Spectrum of 4-*tert*-butylbenzophenone and additional by-products.

DOSY and Variable Temperature NMR Spectroscopic Analysis of 2

The Diffusion-Ordered Spectroscopy (DOSY) NMR experiments were performed on a Bruker AVANCE 400 NMR spectrometer operating at 400.13 MHz for proton resonance under TopSpin (version 2.0, Bruker Biospin, Karlsruhe) and equipped with a BBFO-z-atm probe with actively shielded z-gradient coil capable of delivering a maximum gradient strength of 54 G/cm. Diffusion ordered NMR data was acquired using the Bruker pulse program dstegp3s employing a double stimulated echo with three spoiling gradients. Sine-shaped gradient pulses were used with a duration of 3 ms together with a diffusion period of 100 ms. Gradient recovery delays of 200 μs followed the application of each gradient pulse. Data was accumulated by linearly varying the diffusion encoding gradients over a range from 2% to 95% of maximum for 64 gradient increment values. DOSY plot was generated by use of the DOSY processing module of TopSpin. Parameters were optimized empirically to find the best quality of data for presentation purposes.

At ambient temperature, ^{1}H and ^{13}C NMR spectra of **2** in C_6D_6 solution display two sets of pyridyl resonances and two *t*Bu resonances (Figure S3 and Figure S4), where one set may be expected due to the centre of symmetry of **1** in the solid state. Variable temperature ^{1}H NMR analysis revealed that these resonances coalesce at 320K, whilst cooling to subambient temperature enhances their separation. A variable concentration study (Figure S6 – S9), alongside a DOSY NMR spectrum (Figure S5), suggest the two sets of resonances belong to the same species, hence this effect is likely to be a result of conformational isomerism as opposed to any dimer/monomer equilibrium (refer to DFT calculations for further information).

Table S2 Diffusion coefficients obtained from ^{1}H DOSY NMR experiment.

Chemical Shift (ppm)	Peak Assignment	Diffusion Co-efficient D (10^{-10}) m^2 s^{-1}
7.73	H1-dpa	0.545
6.86	H3-dpa	1.007
6.70	H4-dpa	0.782
6.22	H2-dpa	0.657
1.79	*t*Bu	0.782
1.21	*t*Bu	0.840

DFT Calculations

DFT calculations were performed using the Gaussian computational package G03.[4] In this series of calculations the B3LYP[5] density functionals and the 6-311G(d,p)[6] basis set were used. After each geometry optimisation, a frequency analysis was performed and the energy values quoted include the zero point energy contribution.

[{(dpa)Zn(*t*Bu)}$_2$]

DFT calculations reveal that there is a low energy conformational isomer of **2**, **2A**, arising from rotation of both *t*Bu groups about 180°, which is less stable than model **2** by only 1.69 kcal mol^{-1}. These conformational isomers could be responsible for the two sets of distinct ^{1}H NMR resonances observed at low temperatures.

The formation of another conformational isomer (Figure S18) **2B**, a dimer having a 4-membered (Zn-N)$_2$ ring supplemented by dative Zn-N bonding was also investigated theoretically. This alternative structure bears a strong resemblance to that of the reported compound [Zn(dpa*)(Et)]$_2$ (Fig S18, RHS).[7] DFT calculations revealed this structure to be 10.80 kcal mol^{-1} less stable than **2**. That **2B** is responsible for the second set of resonances observed in the ^{1}H NMR spectrum cannot be unequivocally ruled out. At first glance the pyridine rings of **2B** appear to be non-equivalent. However, in the related complex [Zn(dpa*)(Et)]$_2$ (Figure S18), only one set of pyridyl NMR resonances are observed, suggesting that the pyridyl rings interconvert too rapidly to observe two sets of resonances on the NMR timescale.

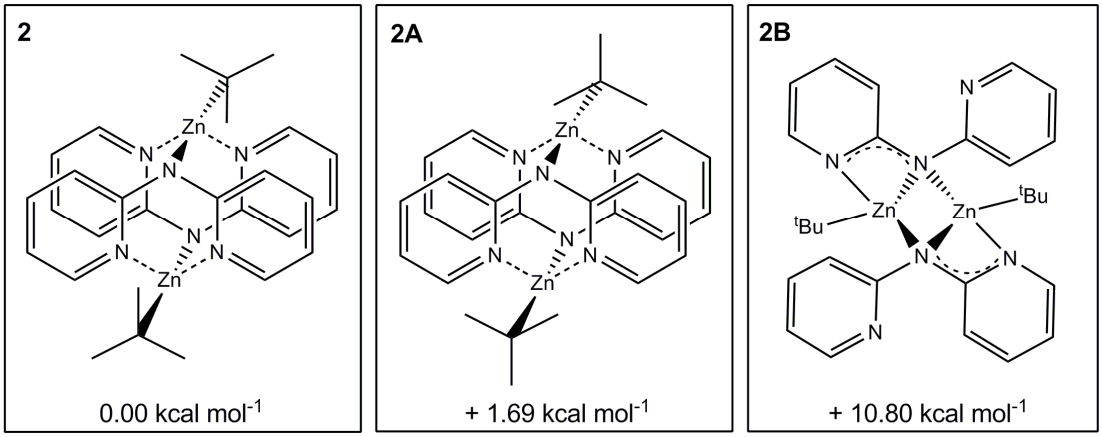

Figure S18 Structure and relative energies of model **2** and conformational isomers **2A** and **2B**.

$[(TMEDA)_2Na_2(\mu\text{-}dpa)_2Zn(tBu)_2]$

Dpa Principal Bond Lengths (Å)

N_1-C_2	1.366	1.362
C_2-N_3	1.363	1.365
N_3-C_4	1.338	1.338
C_4-C_5	1.387	1.387
C_5-C_6	1.400	1.400
C_6-C_7	1.381	1.380
C_7-C_2	1.422	1.425
Na_8-N_1	2.582	
Na_8-$N_{3'}$	2.481	
Na_8-N_{10}	2.577	
Na_8-N_{11}	2.624	
Na_8-N_{12}	2.563	
Na_9-N_1	2.521	
Na_9-N_3	2.466	
Na_9-N_{10}	2.550	
Na_8-N_{13}	2.549	
Na_8-N_{14}	2.582	

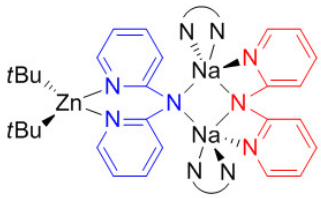

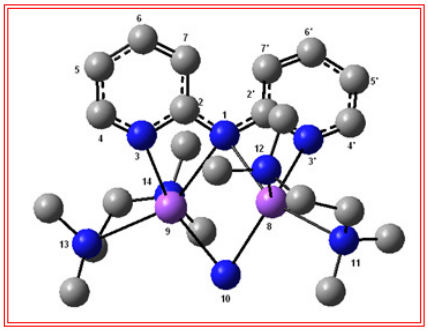

Dpa Principal Bond Angles (˚)

C_2-N_1-$C_{2'}$	122.9
N_1-Na_8-$N_{3'}$	53.9
N_1-Na_9-N_3	54.9
N_1-Na_8-N_{10}	96.9
N_1-Na_9-N_{10}	94.7
Na_8-N_{10}-Na_9	83.7
Na_8-N_1-Na_9	84.2
N_{10}-Na_8-N_{11}	73.5
N_{13}-Na_9-N_{14}	73.4
C_2'-N_1-C_2-C_7	-26.0

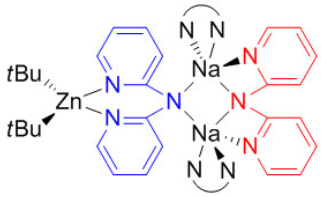

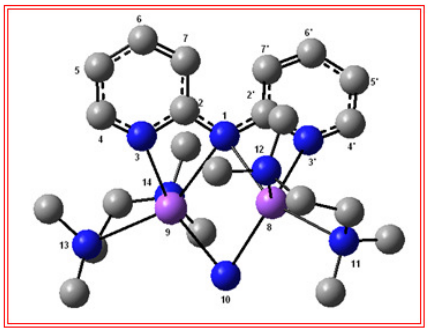

Dpa Principle Bond Indices

N_1-C_2	1.25	1.22
C_2-N_3	1.28	1.29
N_3-C_4	1.40	1.40
C_4-C_5	1.45	1.45
C_5-C_6	1.36	1.37
C_6-C_7	1.51	1.51
C_7-C_2	1.26	1.27
Na_8-N_1	0.02	
Na_8-$N_{3'}$	0.03	
Na_8-N_{10}	0.02	
Na_8-N_{11}	0.02	
Na_8-N_{12}	0.02	
Na_9-N_1	0.02	
Na_9-N_3	0.02	
Na_9-N_{10}	0.02	
Na_8-N_{13}	0.02	
Na_8-N_{14}	0.02	

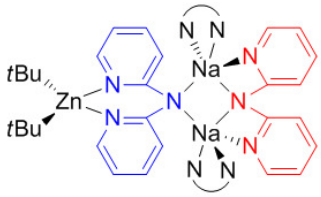

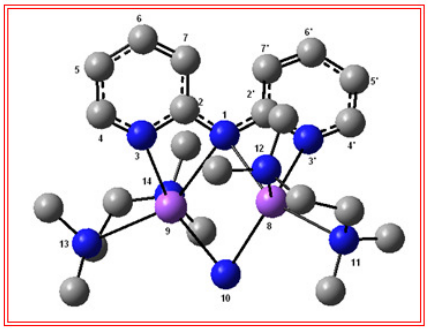

Dpa Charges

N_1	-0.77	
C_2	+0.41	+0.41
N_3	-0.60	-0.60
C_4	+0.08	+0.08
C_5	-0.30	-0.30
C_6	-0.15	-0.15
C_7	-0.31	-0.30
Na_8		+0.88
N_{10}	-0.79	
N_{11}	-0.56	
N_{12}	-0.55	
Na_9		+0.89
N_{13}	-0.55	
N_{14}		-0.56

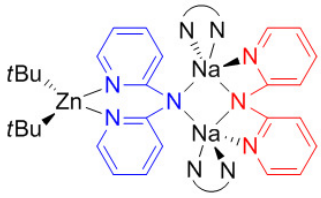

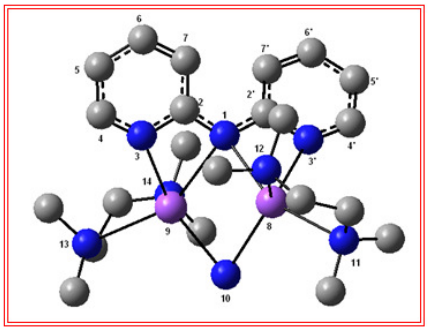

Dpa Principal Bond Lengths (Å) and Angles (˚)

N_{10}-C_2	1.371	1.369
C_2-N_3	1.359	1.360
N_3-C_4	1.346	1.345
C_4-C_5	1.382	1.382
C_5-C_6	1.401	1.400
C_6-C_7	1.377	1.377
C_7-C_2	1.428	1.429
Zn-N_3	2.248	2.252
Zn-C_{15}	2.046	
Zn-C_{16}	2.045	
C_{15}-C_{Me}	1.533, 1.537, 1.536	
C_{16}-C_{Me}	1.533, 1.538, 1.538	
$C_{2''}$-N_{10}-$C_{2'''}$	126.7	
$N_{3''}$–Zn-$N_{3'''}$	80.1	
C_{15}-Zn-C_{16}	134.5	
C_2'-N_1-C_2-C_7	-4.2	

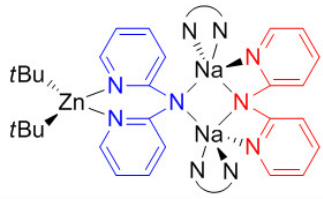

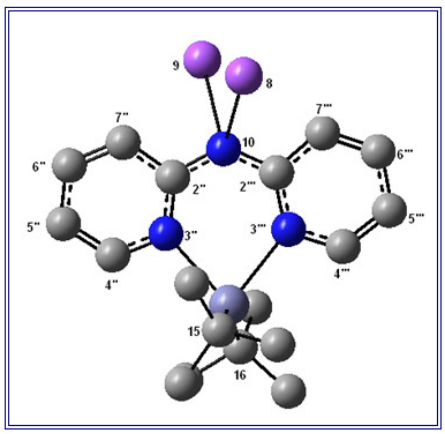

Dpa Principal Bond Indices

N_{10}-C_2	1.23	1.23
C_2-N_3	1.28	1.27
N_3-C_4	1.37	1.36
C_4-C_5	1.47	1.47
C_5-C_6	1.35	1.35
C_6-C_7	1.52	1.52
C_7-C_2	1.27	1.28
Zn-N_3	0.06	0.06
Zn-C_{15}	0.31	
Zn-C_{16}	0.32	
C_{15}-C_{Me}	1.03 1.02 1.02	
C_{16}-C_{Me}	1.03 1.02 1.02	

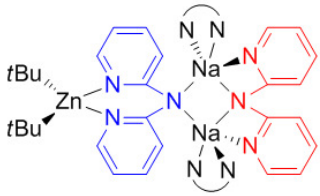

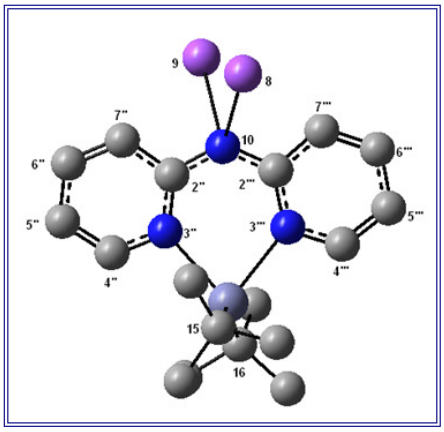

Dpa Charges

N_{10}	-0.79	
C_2	+0.42	+0.42
N_3	-0.63	-0.63
C_4	+0.08	+0.08
C_5	-0.29	-0.29
C_6	-0.16	-0.16
C_7	-0.29	-0.28
Zn	+1.55	
C_{15}	-0.59	
C_{16}	-0.58	
C_{Me}		all -0.59

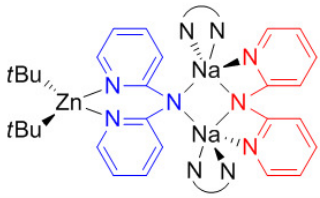

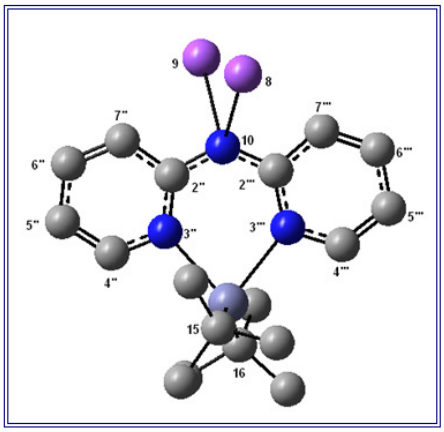

Anion of 4: [Zn(*t*Bu)$_2$(dpa)Zn(*t*Bu)$_2$]

Principal Bond Lengths (Å)

N1-C2	1.363	1.363
C2-N3	1.360	1.359
N3-C4	1.345	1.345
C4-C5	1.380	1.380
C5-C6	1.401	1.401
C6-C7	1.374	1.374
C7-C2	1.429	1.428
Zn1-N1	2.206	
Zn2-N3	2.218	2.216
Zn1-C	2.032	2.026
Zn2-C	2.054	2.050

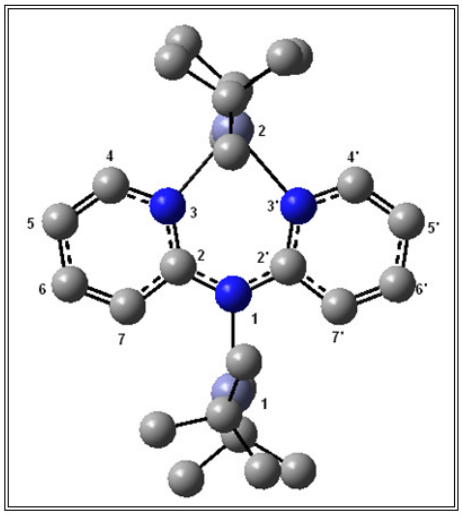

Principal Bond Angles (°)

C_2-N_1-C_2'	127.7
Zn_1-N_1-C_2	116.2 and 115.9
N_3-Zn_2-N_3	81.5
C_2'-N_1-C_2-C_3	1.8

Principal Bond Indices

N1-C2	1.24	1.23
C2-N3	1.27	1.28
N3-C4	1.36	1.36
C4-C5	1.47	1.47
C5-C6	1.34	1.34
C6-C7	1.53	1.53
C7-C2	1.26	1.26
Zn1-N1	0.09	
Zn2-N3	0.06	0.06
Zn1-C	0.34	0.35
Zn2-C	0.30	0.30
C(*t*Bu)-C(Me)	All twelve are 1.03	

Charges

N1	-0.76	
C2	+1.44	+1.44
N3	-0.64	-0.63
C4	+0.08	+0.08
C5	-0.30	-0.30
C6	-0.16	-0.16
C7	-0.26	-0.26
Zn1	+1.47	
Zn2	+1.56	
C(*t*Bu)(Zn1)	-0.57	-0.57
C(*t*Bu)(Zn2)	-0.58	-0.58
C(Me)	All twelve are -0.59	

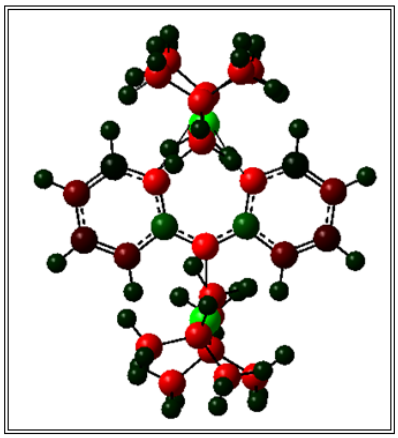

Discussion of Dpa Bond Lengths and Angles

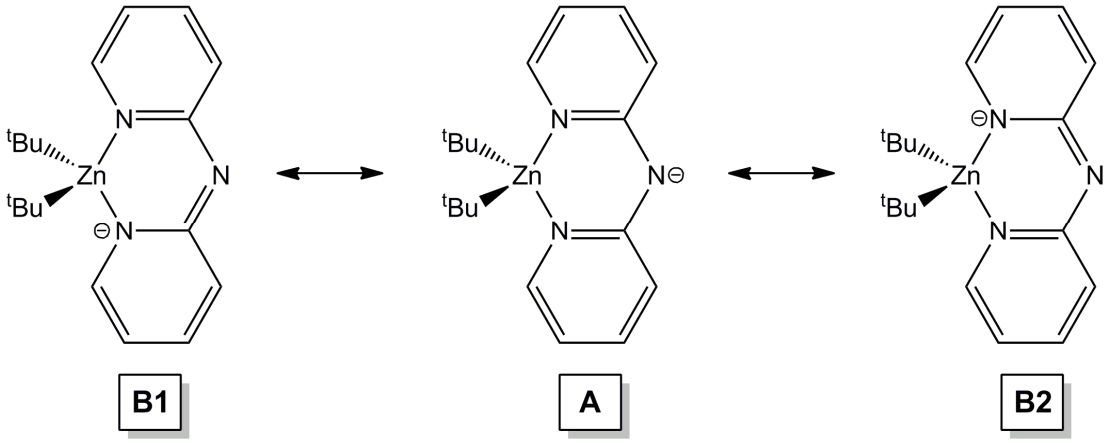

Figure S19 Graphical representation of the resonance delocalisation of dpa.

Through resonance delocalisation, the anionic charge may be focused at the (amido)-N or the (pyridyl)-N (Figure S19). If the anion predominantly lies on the (pyridyl)-N (Figure S19B), this results in a shortened (amido)N-C bond, and elongated (pyridyl)N-C bonds due to the loss of aromaticity. Within Cotton's cobalt complex $[Co(dpa)_2]$,[8] the anionic charge is thought to lie primarily on the (pyridyl)-N, as indicated by the shortened C-(amido)N bond lengths [1.346(4) and 1.344(4) Å] and elongated C-(pyridyl)N bonds [1.367(4) and 1.371(4) Å] (Table S3), in comparison to those of the related compound $[Co\{dpa(H)\}Cl_2]$, with C-(amino)N bond lengths of [1.373(4) and 1.382(4) Å and C-(pyridyl)N bonds of 1.351(4) and 1.348(4) Å].

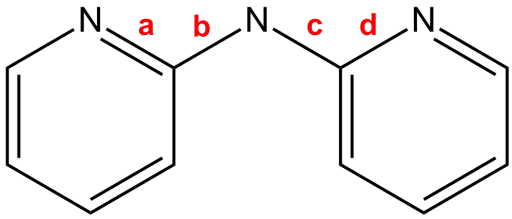

Table S3 Key bond lengths for a range of neutral and anionic dpa complexes.

Compound		**Bond Length (Å)**			
		a	**b**	**c**	**d**
dpa(H) monoclinic	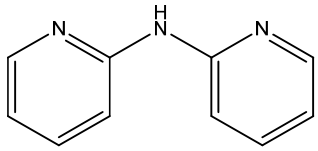	1.343(2)	1.388(2)	1.391(2)	1.335(2)
dpa(H) orthorhombic[9]		1.332(4)	1.379(4)	1.380(4)	1.338(4)
dpa(H) triclinic[10]		1.337(2)	1.380(3)	1.376(3)	1.334(3)
$[Co\{dpa(H)\}Cl_2]$[8]	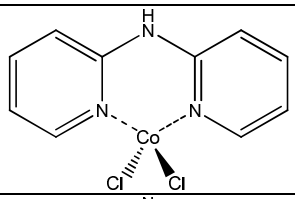	1.351(4)	1.373(4)	1.382(4)	1.348(4)
$[Co(dpa)_2]$[8]	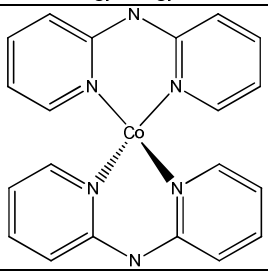	1.367(4)	1.346(4)	1.344(4)	1.371(4)
3	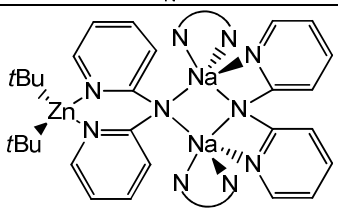	1.347(2)	1.371(2)	1.373(2)	1.346(2)
4[a]	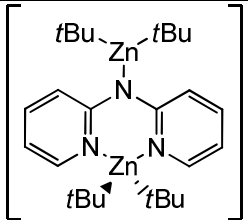	1.360	1.363	1.363	1.359

[a] values taken from DFT calculations.

References

[1] C. Schade, W. Bauer, P. v. R. Schleyer, *J. Organomet. Chem.* **1985**, *295*, C25-C28.

[2] B. Conway, D. V. Graham, E. Hevia, A. R. Kennedy, J. Klett, *Chem. Commun.* **2008**, 2638-2640.

[3] P. C. Andrikopoulos, D. R. Armstrong, H. R. L. Barley, W. Clegg, S. H. Dale, E. Hevia, G. W. Honeyman, A. R. Kennedy, R. E. Mulvey, *J. Am. Chem. Soc* **2005**, *127*, 6184-6185.

[4] M. J. Frisch, G. W. Trucks, H. B. Schlegel, G. E. Scuseria, M. A. Robb, J. R. Cheeseman, J. A. Montgomery, Jr., T. Vreven, K. N. Kudin, J. C. Burant, J. M. Millam, S. S. Iyengar, J. Tomasi, V. Barone, B. Mennucci, M. Cossi, G. Scalmani, N. Rega, G. A. Petersson, H. Nakatsuji, M. Hada, M. Ehara, K. Toyota, R. Fukuda, J. Hasegawa, M. Ishida, T. Nakajima, Y. Honda, O. Kitao, H. Nakai, M. Klene, X. Li, J. E. Knox, H. P. Hratchian, J. B. Cross, V. Bakken, C. Adamo, J. Jaramillo, R. Gomperts, R. E. Stratmann, O. Yazyev, A. J. Austin, R. Cammi, C. Pomelli, J. W. Ochterski, P. Y. Ayala, K. Morokuma, G. A. Voth, P. Salvador, J. J. Dannenberg, V. G. Zakrzewski, S. Dapprich, A. D. Daniels, M. C. Strain, O. Farkas, D. K. Malick, A. D. Rabuck, K. Raghavachari, J. B. Foresman, J. V. Ortiz, Q. B. Cui, A.G., S. Clifford, J. Cioslowski, B. B. Stefanov, G. Liu, A. Liashenko, P. Piskorz, I. Komaromi, R. L. Martin, D. J. Fox, T. Keith, M. A. Al-Laham, C. Y. Peng, A. Nanayakkara, M. Challacombe, P. M. W. Gill, B. Johnson, W. Chen, M. W. Wong, C. Gonzalez, J. A. Pople, *GAUSSIAN03 (Revision C.02)*, Gaussian, Inc.: Wallingford, CT, 2004.

[5] a) W. Kohn, A. D. Becke, R. G. Parr, *J. Phys. Chem.* **1996**, *100*, 12974-12980, b) A. D. Becke, *Phys Rev A* **1988**, *38*, 3098-3100.

[6] a) A. D. Mclean, G. S. Chandler, *J. Chem. Phys.* **1980**, *72*, 5639-5648, b) R. Krishnan, J. S. Binkley, R. Seeger, J. A. Pople, *J. Chem. Phys.* **1980**, *72*, 650-654.

[7] Z. Zheng, M. K. Elmkaddem, C. Fischmeister, T. Roisnel, C. M. Thomas, J.-F. Carpentier, J.-L. Renaud, *New J. Chem.* **2008**, *21*, 2150-2158.

[8] F. A. Cotton, L. M. Daniels, G. T. Jordan IV, C. A. Murillo, *Polyhedron* **1998**, *17*, 589-597.

[9] R. A. Jacobsen, J. E. Johnson, *Acta Crystallogr.* **1973**, *B29*, 1669-1674.

[10] G. J. Pyrka, A. A. Pinkerton, *Acta Crystallogr.* **1990**, *C48*, 91-94.